Proc. Natl. Acad. Sci. USA
Vol. 91, pp. 11924–11928, December 1994
Cell Biology

Coatomer-rich endoplasmic reticulum

LELIO ORCI*, ALAIN PERRELET*, MARIELLA RAVAZZOLA*, MYLÈNE AMHERDT*, JAMES E. ROTHMAN†, AND RANDY SCHEKMAN‡

*Department of Morphology, University of Geneva Medical School, 1211 Geneva 4, Switzerland; ‡Division of Biochemistry and Molecular Biology, Howard Hughes Medical Institute, University of California, Berkeley, CA 94720; and †Cellular Biochemistry and Biophysics Program, Memorial Sloan–Kettering Cancer Center, 1275 York Avenue, New York, NY 10021

Contributed by Randy Schekman, August 30, 1994

ABSTRACT **We identify in normal cells the existence of two distinct sites of the transitional endoplasmic reticulum (ER), one housing the Sec23p protein complex (the classical transitional element), the other the coatomer protein complex (the coatomer-rich ER). Experimental conditions that reduce transport from the ER to the Golgi complex lead to the overexpression of this newly defined coatomer-rich ER.**

Progress in the identification and characterization of the carriers involved in membrane traffic from the endoplasmic reticulum (ER) to and through the Golgi complex was possible by combining morphological and biochemical methods, cell-free assay systems, and yeast genetics (for review see refs. 1–3). Intercompartmental transport in eukaryotes is thought to involve the production of coated vesicle intermediates from a donor compartment that uncoat prior to fusion with an acceptor compartment (for review, see refs. 2 and 3). Well-characterized examples of coated vesicular carriers are clathrin-coated vesicles derived from the plasma membrane and from the trans-Golgi network (for review see ref. 4), and non-clathrin-coated vesicles that are involved in intra-Golgi transport (5–9). Coatomer (for coat protomer) (10) in non-clathrin-coated Golgi transport vesicles is a complex of several distinct protein subunits called COP (11–16). Recently, budding of vesicles for ER-to-Golgi transport in yeast has been shown to be mediated by Sec23p and members of another coat protein complex, named COPII (17). The mammalian equivalents of Sec23p (18, 19) and Sec13p (D. Shaywitz, L.O., M.R., M. Swaroop, and C. A. Kaiser, unpublished data) are enriched in the transitional region of the ER, comprising budding profiles of the transitional cisternae, transfer vesicles, and surrounding cytosolic matrix.

The ER–Golgi region is profoundly disorganized by treatment with brefeldin A (BFA) (for review see ref. 21). In the pancreatic acinar cell, BFA induces spherical aggregates of β-COP subunits of coatomer associated with ribosome-free ends of ER cisternae (22, 23). In the pancreatic insulin cell, BFA treatment results in the accumulation of coatomer-rich pairs of ER cisternae, or stacks of pairs, called the BFA bodies (19). In these bodies, one of the cisternae is transitional and coatomer is present on the smooth (ribosome-free) cisternal face opposite to that giving rise to buds and transfer vesicles marked characteristically by Sec23p (19). We now report the occurrence in normal cells of an ER domain segregating coatomer from Sec23p and demonstrate that this compartment can reversibly be expanded by lowering the temperature to below 37°C. We refer to this newly defined domain of the ER as the coatomer-rich ER (CRER).

MATERIALS AND METHODS

Tissue Preparation. Pancreatic islets of normal adult rats (SIVZ and Wistar strains) were isolated by collagenase digestion and incubated at normal (37°C) or low (22°C, 15°C, 4°C) temperatures under continuous shaking and gassing with 95% O_2/5% CO_2. Monolayer cultures of pancreatic endocrine cells (24) were exposed to low temperatures as for isolated islets. ATP depletion in both preparations was induced at 37°C with 10 μM antimycin or 1 mM dinitrophenol or by gassing the cells with N_2 instead of the O_2/CO_2 mixture.

At the end of the incubations, the samples were fixed with 1% glutaraldehyde in 0.1 M sodium phosphate buffer (pH 7.4) for 1 hr at the final temperature of the incubation protocol, washed with buffer, and processed for Epon embedding (conventional thin sections) or for cryoultramicrotomy according to Tokuyasu (25) (thin cryosections). Insulin cells from islets of pancreas fixed by perfusion (26) were also examined.

Conventional thin sections were sequentially stained with uranyl acetate and lead citrate and examined in a Philips electron microscope.

Immunocytochemistry. Thin cryosections were collected on nickel grids and processed by the protein A–gold technique (27) for single labeling with either anti-Sec23p, anti-β-COP (anti-EAGE; a gift from T. Kreis, Department of Cell Biology, University of Geneva, Switzerland), or ε-COP antibodies as described (19). For double labeling, rabbit anti-Sec23p antibody was visualized with goat anti-rabbit IgG conjugated to 15-nm gold particles (GAR15); monoclonal anti-β-COP antibody (M3A5; a gift from T. Kreis) was revealed with goat anti-mouse IgG conjugated to 5-nm gold particles (GAM5). GAR15 and GAM5 were purchased from Aurion (Wageningen, The Netherlands). After the immunolabeling, the sections were washed with distilled water, absorption-stained with uranyl acetate, and photographed in a Philips electron microscope.

The size of the CRER compartment in the insulin cells exposed to the various experimental conditions was measured by a standard morphometric procedure (28).

RESULTS

Fig. 1*a* shows a conventional thin section of an insulin cell incubated at low temperature, a condition that best reveals the typical cisternal pair characterizing CRER. It consists of a band of ribosome-free cytosol along a classical transitional cisterna, on the side opposite to that giving rise to buds and vesicles. This band is bordered by another ER cisterna, smooth on the side in contact with the dense cytosol, and dotted with ribosomes on the other side. The intercisternal space has a regular width but can extend from a fraction of a micrometer to up to 2 μm. This arrangement was also found in cells fixed at normal temperature (Figs. 1*e* and 2*a*). The cisternal pair described is analogous to the simplest form of the BFA body, consisting of coatomer sandwiched between two ER cisternae, one of them classically transitional and

The publication costs of this article were defrayed in part by page charge payment. This article must therefore be hereby marked "*advertisement*" in accordance with 18 U.S.C. §1734 solely to indicate this fact.

Abbreviations: ER, endoplasmic reticulum; CRER, coatomer-rich ER; BFA, brefeldin A.

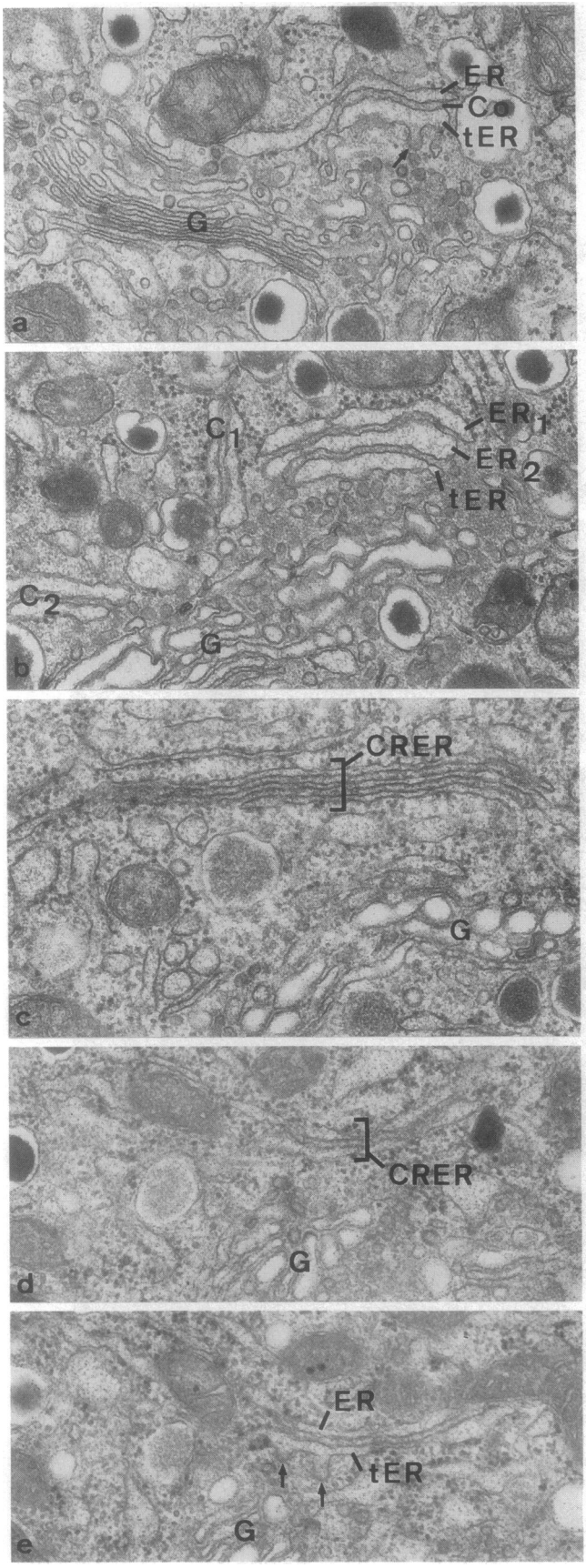

FIG. 1. Examples of the spectrum of different morphologies taken by CRER in insulin cells. (*a*) Insulin cell incubated at 15°C shows typical paired cisternae formed by a band of cytosolic matrix (Co) sandwiched between a part rough, part smooth ER cisterna (ER), and a classical transitional cisterna (tER) with a budding profile (arrow); G, Golgi complex. (*b*) Insulin cell incubated at 4°C shows the same morphology as in *a*, but with an additional smooth ER cisterna (ER_2) interposed in the middle of the paired cisternae delimited by ER_1 and tER. CR_1 and CR_2 are two additional CRERs. (*c*) Insulin cell fixed *in situ* by perfusion shows CRER in a cytoplasmic position not indicative of a relationship with the Golgi. Such images are numerous in the literature and many of them were unnoticed; these can now be interpreted as CRER. (*d*) Insulin cell fixed at normal temperature shows inconspicuous CRER that appears as a typical cisternal pair (ER, tER) on the next consecutive serial section (*e*). The arrows in *e* indicate budding profiles from tER. These images point to the possible difficulty in identifying CRER on random sections. See also legend of Fig. 2*d*. Although any of the sizes/shapes of CRER illustrated can be found in normal cells, low-temperature incubation increases the probability of forms seen in *a* and *b*. See Table 1 for the quantitation of CRER in the different conditions studied. (*a–c* ×33,600; *d* and *e*, ×33,400.)

marked by Sec23p (19). In addition to the typical transitional–nontransitional ER cisternal pair, there were pairs in which the ribosome-free band of cytosol was sandwiched between two cisternae with a nontransitional appearance (Fig. 1*d*). This is due to the fact that the pairing of cisternae might extend well beyond the circumscribed transitional area.

By shifting the cells to temperatures below 37°C, the formation of such cisternal pairs was amplified in number and size. The basic cisternal pair could be enlarged by additional (up to three) smooth cisternae bordered on each side by a band of dense cytosol (Figs. 1*b* and 3). This expansion was observed at temperatures between 20°C and 30°C, although the most prominent effect was seen between 4°C and 15°C and also during ATP depletion (Table 1). Expansion of paired cisternae was also observed in AtT-20 mouse pituitary tumor cells at temperatures between 4°C and 15°C (data not shown). Recovery from low-temperature incubation to 37°C indicated that the process was completely reversible. A serial sectioning study on conventional sections was performed to quantify the frequency of cisternal pairs in normal insulin cells. On several independent series of consecutive thin sections, we found cisternal pairs in >70% of the cells.

On cryosections of comparable material fixed at normal or low temperatures, the cytosolic band in the middle of the cisternal pairs stained specifically for coatomer (Fig. 2 *b–g*). Cisternal pairs containing coatomer were found in a range of cells, including endocrine cells of the islet of Langerhans other than insulin cells, prolactin cells of the pituitary, neurons from the cerebral cortex, CHO and NRK cells, and an erythroleukemia cell line. This coatomer-segregating compartment seems thus to be a normal component of cells, although its degree of extension might be quite variable (*cf.* Fig. 1 *c* and *d*).

Since buds were not evident on the coatomer-rich cisternae, we assessed coatomer and Sec23p labeling on those membrane buds present on classically transitional elements facing the cis-Golgi compartment and at the peripheral rim of Golgi cisternae. While on average 58% of the buds occurring at the peripheral rim of Golgi cisternae were labeled by β- or ε-COP, only about 8% of the buds on transitional cisternae appeared coatomer-positive. Sec23p staining was found on 52% of the buds on transitional ER elements, compared with only 3% for those at the peripheral rim of Golgi cisternae (Table 2). The low percentage of coatomer labeling on transitional buds, and of Sec23p labeling on buds at the peripheral rim of Golgi cisternae, may represent nonspecific background, since all buds with at least one immunogold particle were included. That coatomer-coated buds were virtually absent raises the question of the origin of coatomer-coated vesicles in the transitional region (19 and 22). At present, we interpret them as vesicles belonging to the peripheral rim of the Golgi cisternae intermixed with Sec23p-positive vesicles.

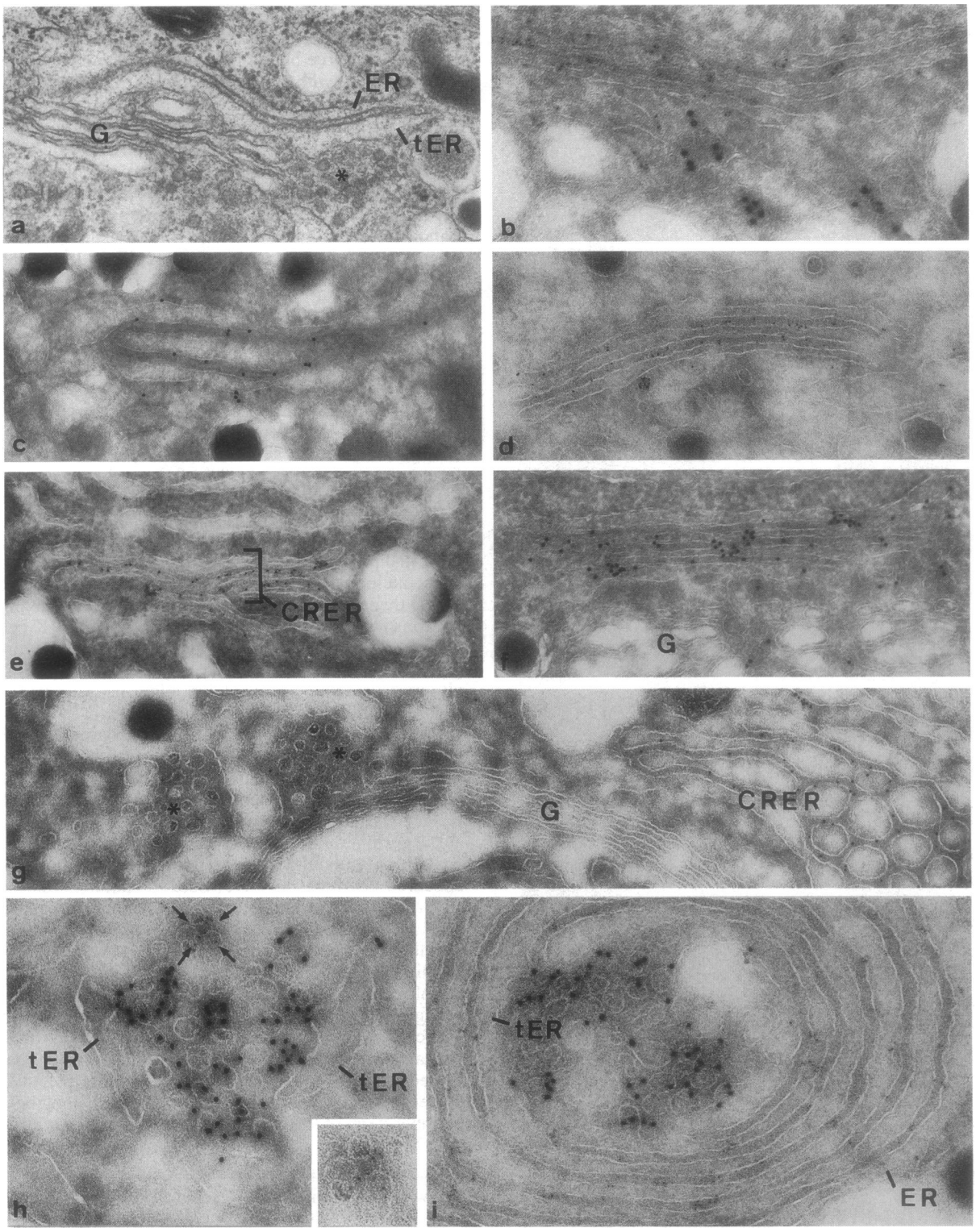

FIG. 2. Example of immunolabeled CRERs on thin cryosections. (*a*) Insulin cell fixed at normal temperature shows a typical cisternal pair (ER, tER) juxtaposed to the Golgi complex (G). Asterisk indicates transfer vesicles. (*b*) Insulin cell fixed *in situ* by perfusion shows an area similar to that in *a* after double immunolabeling using 5-nm gold particles to label β-COP and 15-nm gold particles to label Sec23p. Note the clear topological segregation of the two gold markers. (*c*) β-COP labeling of an insulin cell incubated at 15°C. (*d*) ε-COP labeling of an insulin cell fixed *in situ* by perfusion. Without coatomer immunolabeling, such an image could be misinterpreted as stacked Golgi cisternae. (*e*) ε-COP labeling of an insulin cell incubated for 60 min at 37°C in 16.7 mM glucose. (*f*) ε-COP-rich CRER juxtaposed to Golgi cisternal elements (G) in an insulin cell incubated for 30 min at 15°C. (*g*) Unusually developed CRER in an insulin cell incubated for 60 min at 37°C in 1.67 mM glucose. Note the clear topological segregation of the coatomer-rich (ε-COP) elements (both cisternal and tubular) from the classical transitional region with transfer vesicles (asterisks). G, Golgi stack. (*h*) Least characteristic form of morphologic segregation of β-COP (5-nm gold particles) from Sec23p-positive (15-nm gold particles) transitional cisternae (tER) and associated vesicles; the β-COP-rich elements (arrows) are shown at high magnification (*Inset*). (*i*) Most characteristic form of segregation of β-COP (5-nm gold) from Sec23p (15-nm gold) in a typical BFA body made of several superimposed paired cisternae. ER, ER cisterna delimiting the outermost face of the BFA body; tER, transitional cisternae on the innermost side. [*b*, *h*, and *i* show goat anti-rabbit (15-nm gold)/goat anti-mouse (5-nm gold) labeling; *c*, *d*, *e*, *f*, and *g* show protein A–gold labeling; *a*, ×33,000; *b*, ×66,200; *c*, ×49,400; *d*, ×41,400; *e*, ×31,400; *f*, ×41,400; *g*, ×40,200; *h*, ×57,000 (*Inset*, ×88,700); *i*, ×46,200.]

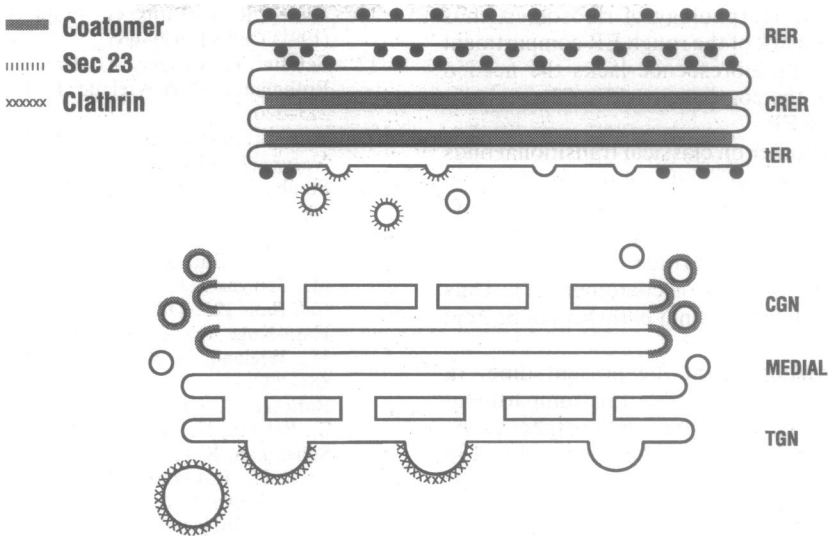

FIG. 3. Highly schematized drawing of the respective distribution of coatomer, Sec23p, and clathrin on the ER and Golgi compartments. The interconnected and ramified pattern of ER cisternae has not been represented. RER, rough ER; tER, classical transitional cisterna of the ER; CGN, cis-Golgi network; TGN, trans-Golgi network.

On most cisternal pairs, the segregation of coatomer-positive domains from Sec23p-labeled fronts was evident; however, there were images in which coatomer-labeled structures were more difficult to resolve from the Sec23p compartment. In these cases, we used a double-labeling technique with the respective secondary antibodies (IgG) directly coupled to gold particles of distinct sizes. Fig. 2*h* shows that the Sec23p and β-COP immunoreactive sites did not colocalize. Fig. 2*i* shows an example of double labeling of a typical BFA body. The schematic arrangement of coatomer and Sec23p compartments is drawn in Fig. 3. In cells with poorly developed ER (e.g., erythroleukemia cells), a diminutive equivalent of CRER can be traced at the level of the nuclear envelope (data not shown).

DISCUSSION

Through a comparative approach using conventional and immunolabeled cryosections, we have identified in normal insulin cells two topologically distinct sites of the transitional ER, one labeled by Sec23p (the classically transitional buds and vesicular profiles), the other labeled with the coatomer protein complex (the CRER). This basic arrangement forms a cisternal pair in which coatomer is proximal (or lateral, depending on the section plane) to the Sec23p positive front. In the normal acinar pancreatic cell, Oprins *et al.* (22) have reported that β-COP and Sec23p do not colocalize, but indicated (see figure 9 in their paper) that coatomer-coated buds and coatomer-coated vesicles emerge from the transitional cisternal membrane domain labeled with Sec23p. The difference in interpretation between their and our data might stem from the fact that the rat exocrine cells lack the typical CRER morphology described here. The exocrine cells also react differently to BFA treatment, which induces spherical aggregates of coatomer surrounded by ribosome-free ends of ER cisternae (22, 23), rather than coatomer bands sandwiched between paired ER cisternae (19).

Cisternal pairs have previously been described, most frequently in mitotic or virus-infected cells (see for example figure 13 in ref. 29, figure 3 in ref. 30, figure 1 in ref. 31, and figures 7 and 12 in ref. 32). Inspection of the numerous published pictures of the ER–Golgi region in various cell types also reveals, retrospectively, the occurrence of typical cisternal pairs. Since all these previously published pictures lack the immunocytochemical coatomer marker, and most of them are devoid of the topological marker represented by the cis-Golgi compartment, their exact identity as CRERs remains unsettled. However, we believe that many of them (if not all) do represent various forms of CRER. In the more recent immunocytochemical era, paired cisternae, or stacks of such pairs, can easily be misattributed to the Golgi complex if coatomer staining is not used, because the preparation procedures for detection of antigens (i.e., cryoultra-

Table 1. Volume density of CRER in insulin cells

Condition	CRER volume density, Vv × 10^2	Time, min	Glucose, mM	No. of cells measured
Isolated islets				
37°C	0.18 ± 0.06	60	16.7	48
22°C	1.21 ± 0.21	60	16.7	32
15°C	4.54 ± 0.38	60	16.7	48
4°C	6.79 ± 0.39	60	16.7	48
Antimycin (10 μM)	5.19 ± 0.64	15	1.67	24
Dinitrophenol (1 mM)	4.36 ± 0.81	60	1.67	24
Control	0.38 ± 0.16	60	1.67	24
Nitrogen	4.09 ± 0.53	30	16.7	24
Control	0.20 ± 0.07	30	16.7	24
Monolayer cultures				
20°C	1.13 ± 0.33	60	16.7	30
15°C	1.93 ± 0.34	60	16.7	30
4°C	4.35 ± 0.32	60	16.7	30

Data were collected on conventional thin sections (see Fig. 1).

Table 2. β-COP, ε-COP, and Sec23p labeling of budding profiles from Golgi cisternae and ER transitional elements in insulin cells

	% of labeled buds	
Labeling	Golgi cisternae (lateral rim)	ER transitional elements
β-COP	60 (132)	9 (188)
ε-COP	55 (132)	6 (71)
Sec23p	3 (77)	52 (151)

Buds showing at least one gold particle on the limiting membrane were considered labeled. The total number of buds evaluated is shown in parentheses. Data were collected on cryosections immunolabeled with anti-COP or anti-Sec23p antibodies revealed by the protein A–gold technique.

microtomy), often blur the morphology of ribosomes, thus eliminating a valuable hallmark of the rough ER compartment (e.g., see Fig. 2*d*). Immunofluorescence lacks the needed resolution to discriminate the coatomer and Sec23p segregation that characterizes CRER.

That we do not find coatomer on classical transitional buds and vesicles is difficult to reconcile with the data on coatomer-dependent ER-to-Golgi transport (33–35). However, vesicle budding mediated by Sec23p and members of another coat protein complex (COPII) has been reproduced in a purified system that is devoid of coatomer (17). Thus coatomer and COPII may define distinct pathways of protein transport from the ER.

CRER has no known function at the present time. In particular, there are no clues as to whether this compartment behaves as donor or acceptor (or neither) with respect to the cis-Golgi compartment. The fact that CRER is amplified in conditions that reduce or block ER to Golgi transport suggests that this coatomer pool can be used in transport. The binding to coatomer of dilysine endoplasmic reticulum retention motifs was recently described (20), and a possible role of coatomer in retrograde, Golgi-to-ER transport was suggested. According to this view, the coatomer-rich compartment would sort dilysine-tagged proteins in vesicles/tubules destined to be returned to the ER. It seems also possible that coatomer–dilysine interaction could help retain ER proteins in CRER domains.

This work was supported by grants from the Swiss National Science Foundation (L.O.), the Human Frontier Science Program (J.E.R. and L.O.), and the Howard Hughes Medical Institute (R.S.).

1. Palade, G. E. (1975) *Science* **189,** 347–358.
2. Pryer, N. K., Wuestehube, L. J. & Schekman, R. (1992) *Annu. Rev. Biochem.* **61,** 471–516.
3. Rothman, J. E. & Orci, L. (1992) *Nature (London)* **355,** 409–415.
4. Pearse, B. S. & Robinson, M. L. (1990) *Annu. Rev. Cell Biol.* **6,** 151–171.
5. Orci, L., Glick, B. S. & Rothman, J. E. (1986) *Cell* **46,** 171–184.
6. Orci, L., Malhotra, V., Amherdt, M., Serafini, T. & Rothman, J. E. (1989) *Cell* **56,** 357–368.
7. Melançon, P., Glick, B. S., Malhotra, V., Weidman, P. J., Serafini, T., Gleason, M. L., Orci, L. & Rothman, J. E. (1987) *Cell* **51,** 1053–1062.
8. Malhotra, V., Serafini, T., Orci, L., Shepherd, J. C. & Rothman, J. E. (1989) *Cell* **58,** 329–336.
9. Osterman, J., Orci, L., Tani, K., Amherdt, M., Ravazzola, M., Elazar, Z. & Rothman, J. E. (1993) *Cell* **75,** 1015–1025.
10. Waters, M. G., Serafini, T. & Rothman, J. E. (1991) *Nature (London)* **349,** 248–251.
11. Duden, R., Griffiths, G., Frank, R., Argos, P. & Kreis, T. E. (1991) *Cell* **64,** 649–665.
12. Serafini, T., Stenbeck, G., Brecht, A., Lottspeich, L., Orci, L., Rothman, J. E. & Wieland, F. T. (1991) *Nature (London)* **349,** 215–220.
13. Orci, L., Palmer, D. J., Amherdt, M. & Rothman, J. E. (1993) *Nature (London)* **364,** 732–734.
14. Stenbeck, G., Harter, C., Brecht, A., Herrmann, D., Lottspeich, F., Orci, L. & Wieland, F. T. (1993) *EMBO J.* **12,** 2841–2845.
15. Kuge, O., Hara-Kuge, S., Orci, L., Ravazzola, M., Amherdt, M., Tanigawa, G., Wieland, F. T. & Rothman, J. E. (1993) *J. Cell Biol.* **123,** 1727–1734.
16. Hara-Kuge, S., Kuge, O., Orci, L., Amherdt, M., Ravazzola, M., Wieland, F. & Rothman, J. E. (1994) *J. Cell Biol.* **124,** 883–892.
17. Barlowe, C., Orci, L., Yeung, T., Hosobuchi, M., Hamamoto, S., Salama, N., Rexach, M., Ravazzola, M., Amherdt, M. & Schekman, R. (1994) *Cell* **77,** 895–908.
18. Orci, L., Ravazzola, M., Meda, P., Holcomb, C., Moore, H.-P., Hicke, L. & Schekman, R. (1991) *Proc. Natl. Acad. Sci. USA* **88,** 8611–8615.
19. Orci, L., Perrelet, A., Ravazzola, M., Wieland, F. T., Schekman, R. & Rothman, J. E. (1993) *Proc. Natl. Acad. Sci. USA* **90,** 11089–11093.
20. Cosson, P. & Letourneur, F. (1994) *Science* **263,** 1629–1631.
21. Klausner, R. D., Donaldson, J. G. & Lippincott-Schwartz, J. (1992) *J. Cell Biol.* **116,** 1071–1080.
22. Oprins, A., Duden, R., Kreis, T. E., Geuze, H. J. & Slot, J. W. (1993) *J. Cell Biol.* **121,** 49–59.
23. Hendricks, L., McCaffery, M., Palade, G. E. & Farquhar, M. G. (1991) *Mol. Biol. Cell* **4,** 413–424.
24. Orci, L., Like, A. A., Amherdt, M., Blondel, B., Kanazawa, Y., Marliss, E. B., Lambert, A. E., Wolheim, C. B. & Renold, A. E. (1973) *J. Ultrastruct. Res.* **43,** 270–297.
25. Tokuyasu, K. T. (1980) *Histochem. J.* **12,** 381–403.
26. Forssmann, W. G., Siegrist, G., Orci, L., Girardier, L., Pictet, R. & Rouiller, Ch. (1967) *J. Microsc.* **6,** 279–304.
27. Roth, J., Bendayan, M. & Orci, L. (1978) *J. Histochem Cytochem.* **26,** 1074–1078.
28. Weibel, E. R. (1979) *Stereological Methods* (Academic, London), Vol. 1, pp. 1–415.
29. Sato, S., Murphy, G. F. & Harrist, T. J. (1982) *Am. J. Pathol.* **107,** 150–160.
30. Tooze, J., Tooze, S. A. & Warren, G. (1985) *Eur. J. Cell Biol.* **36,** 108–115.
31. Palisano, J. R. (1993) *Cell Biol. Int. Rep.* **17,** 653–664.
32. Walter, R. J. & Tandler, B. (1989) *J. Submicrosc. Cytol. Pathol.* **21,** 93–101.
33. Hosobuchi, M., Kreis, T. K. & Schekman, R. (1992) *Nature (London)* **360,** 603–606.
34. Peter, F., Plutner, H., Zhu, H., Kreis, T. E. & Balch, W. E. (1993) *J. Cell Biol.* **122,** 1155–1167.
35. Pepperkok, R., Scheel, J., Horstmann, H., Hauri, H. P., Griffiths, G. & Kreis, T. E. (1993) *Cell* **74,** 71–82.